

Numerical estimates of square lattice star vertex exponents

S Campbell¹ and EJ Janse van Rensburg²

¹*Department of Statistics, University of Toronto, Toronto, Ontario M3J 4S5, Canada*

²*Department of Mathematics and Statistics, York University, Toronto, Ontario M3J 1P3, Canada*

Email: rensburg@yorku.ca

(Dated: March 19, 2021)

We implement parallel versions of the GARM and Wang-Landau algorithms for stars and for acyclic uniform branched networks in the square lattice. These are models of monodispersed branched polymers, and we estimate the star vertex exponents σ_f for f -stars, and the entropic exponent $\gamma_{\mathcal{G}}$ for networks with comb and brush connectivity in two dimensions. Our results verify the predicted (but not rigorously proven) exact values of the vertex exponents and we test the scaling relation [5]

$$\gamma_{\mathcal{G}} - 1 = \sum_{f \geq 1} m_f \sigma_f$$

for the branched networks in two dimensions.

PACS numbers: 82.35.Lr, 82.35.Gh, 61.25.Hq

INTRODUCTION

The vertex exponents of lattice star models of monodispersed branched polymers have been studied since the 1970s. These exponents have been estimated numerically in numerous studies [1, 8–10, 12, 17, 18, 26, 28]. Theoretical approaches can be found in references [5, 6, 11, 13, 14, 21]. Recent results in reference [7] make various predictions in models of confined star polymers.

In this paper we use a parallel implementation of the flatGARM algorithm [2] to estimate two dimensional values of the star vertex exponents. In addition, we use a parallel implementation of the Wang-Landau algorithm [25, 29–31] to estimate the entropic exponents of monodispersed acyclic branched networks in the square lattice. In particular, we test the scaling relation [5]

$$\gamma_{\mathcal{G}} - 1 = \sum_{f \geq 1} m_f \sigma_f \quad (1)$$

where \mathcal{G} is the connectivity of the branched network (see figure 1). This relates the entropic exponent $\gamma_{\mathcal{G}}$ of the network to the star vertex exponents σ_f .

In our implementation of flatGARM we sampled square lattice f -stars to lengths 1000 steps (edges) per arm, for $f \in \{3, 4, 5, 6\}$. Monodispersed branch networks (a comb and two brushes) with underlying connectivity shown in figure 1 were sampled using the Wang-Landau algorithm to lengths of 200 steps per branch.

The branches (arms) of lattice stars and monodispersed branched networks (figure 1) are self-avoiding walks (also avoiding each other) joining nodes of various degrees. In an f -star, the branches join the central node of degree f to f nodes of degree 1, and the total length of the star is fn , if each branch has length n . Similarly, the length of a uniform network consisting of b branches

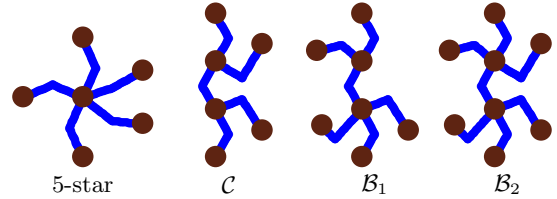


FIG. 1: From the left, schematic diagrams of the connectivity of a 5-star, a comb \mathcal{C} , a brush \mathcal{B}_1 , and a brush \mathcal{B}_2 .

each of length n is bn , and the branches are self-avoiding walks joining the nodes in the network.

A lattice f -star is *almost uniform* if the length of the longest arms exceed the length of the shortest arms by exactly one. If the arms have the same length, then it is *uniform*. A lattice star will be *monodispersed* if it is uniform, or almost uniform. Uniform, almost uniform and monodispersed branched networks are similarly defined.

Denote by $s_n^{(f)}$ the number of monodispersed lattice stars of total length n , and with f arms. The *growth constant* μ_2 is defined by

$$\lim_{n \rightarrow \infty} \frac{1}{n} \log s_n^{(f)} = \log \mu_2. \quad (2)$$

This limit is known to exist in d -dimensions [22–24, 26, 27] for uniform f -stars (that is, if $n = fm$ as $m \rightarrow \infty$), and μ_d is equal to the growth constant of self-avoiding walks. The methods in references [23, 26] can also be used to prove this for monodisperse lattice f -stars. We classify monodisperse lattice f -stars of length $n = fm + k$ according to the remainder $k \in \{0, 1, 2, \dots, f-1\}$. Uniform stars are in the class $k = 0$ while almost uniform stars are in the classes with $1 \leq k < f$.

Denote by c_n the number of self-avoiding walks from

the origin. There is substantial numerical evidence that

$$c_n = C n^{\gamma-1} \mu_2^n (1 + o(1)) \quad (3)$$

where γ is the entropic exponent. In two dimensions $\gamma = 43/32$ is exact [15, 16]. In analogy with equation (3) the asymptotic behaviour of $s_n^{(f)}$ is

$$s_{mf+k}^{(f)} = C_k^{(f)} n^{\gamma_f-1} \mu_2^n (1 + o(1)), \quad (4)$$

in the square lattice, where k is fixed in $\{0, 1, 2, \dots, f-1\}$ and where $n = fm+k$, and μ_2 is the self-avoiding square lattice growth constant. Only the amplitude $C_k^{(f)}$ is dependent on the class of monodispersed stars, while the entropic exponent γ_f is dependent only on the number of arms. Parity effects in $s_n^{(f)}$ (due to both the lattice, and the number of arms f) are present in the $o(1)$ correction term, and so decay with increasing n .

Equations (2) and (4) can be generalised to square lattice stars with $f > 4$ arms by using more than one central node as shown in figure 2. The edge joining the two central nodes does not count towards the total length of the star.

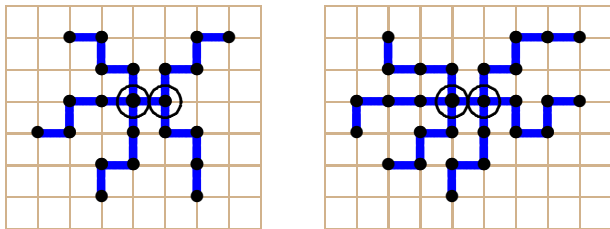


FIG. 2: A uniform square lattice 5-star and a 6-star. There are two central nodes accommodating the arms. Since the edge joining the two central nodes is not counted as part of the length of the star, then 5-star on the left has length 20, and the 6-star on the right has length 24.

The entropic exponent γ_f of f -stars is related to *vertex exponents* σ_f by [5, 6]

$$\gamma_f - 1 = \sigma_f + f \sigma_1. \quad (5)$$

More generally, the vertex exponents are associated with nodes in stars and more general monodispersed branched networks: σ_1 is associated with end-vertices of degree 1 (end-points of branches), while the σ_f with $f \geq 3$ are associated with nodes of degree f in the networks. If $f = 1$, then γ_1 is the entropic exponent γ of self-avoiding walks, with exact value $\gamma_1 = 43/32$ in two dimensions [15, 16]. By equation (5), $\sigma_1 = 11/64$. If $f = 2$, then the star has two arms and so is a self-avoiding walk. This shows by equation (5) that $\sigma_2 = 0$. Exact values for the other vertex exponents are similarly calculated from equation (5) and are given by [5, 15, 16]

$$\sigma_f = \frac{1}{16} + \frac{1}{4} f - \frac{9}{64} f^2. \quad (6)$$

We show the exact values and estimates of σ_f in two dimensions for $f \leq 6$ in table I, and compare it to the results in reference [28], and with the values obtained in this paper. Our results confirm to within numerical accuracy the exact values.

TABLE I: Vertex exponents in 2 dimensions

f	Exact	[28]	This work
σ_1	0.171875	–	0.17188(12)
σ_3	-0.453125	-0.45(2)	-0.45282(69)
σ_4	-1.1875	-1.17(4)	-1.1864(27)
σ_5	-2.203125	-2.14(4)	-2.2016(19)
σ_6	-3.5	-3.36(5)	-3.4981(27)

Lattice networks are *uniform* if all their branches are self-avoiding walks of the same length m . If a uniform lattice network of connectivity \mathcal{G} has b branches and $n = bm$ edges, then the total number of such networks (up to equivalency under translations) is denoted by $c_n(\mathcal{G})$. It is generally accepted that

$$c_n(\mathcal{G}) = C_{\mathcal{G}} n^{\gamma_{\mathcal{G}}-1} \mu_2^n (1 + o(1)), \quad (7)$$

where the growth constant is equal to that of square lattice self-avoiding walks [22–24, 27]. The relation of $\gamma_{\mathcal{G}}$ to the vertex exponents is given by

$$\gamma_{\mathcal{G}} - 1 = \sum_{f \geq 1} m_f \sigma_f - c(\mathcal{G}) d\nu, \quad (8)$$

where m_f is the number of vertices of degree f , and where $c(\mathcal{G})$ is the cyclomatic index (the number of independent cycles) in the network [5, 6]. The networks in figure 1 are acyclic, and by the above

$$\begin{aligned} \gamma_{\mathcal{C}} - 1 &= 4\sigma_1 + 2\sigma_3, \\ \gamma_{\mathcal{B}_1} - 1 &= 5\sigma_1 + \sigma_3 + \sigma_4, \\ \gamma_{\mathcal{B}_2} - 1 &= 6\sigma_1 + 2\sigma_4. \end{aligned} \quad (9)$$

The exact values of the $\gamma_{\mathcal{G}}$ are obtained from these relations assuming that the scaling relation in equation (8) holds, and are listed in the second column of table II. In the third column we list estimates obtained using equation (9) and the numerical estimates listed in table I, and in the last column the direct estimates from our Wang-Landau data for lattice networks. These results show excellent agreement with both the exact values and the numerical data using equation (9) which is strong numerical evidence that equation (9) applies to the branched polymer networks shown in figure 1.

NUMERICAL SIMULATIONS

Determining σ_1

The numbers c_n in equation (3) were estimated by sampling self-avoiding walks to length 10,000 with the paral-

TABLE II: $\gamma_{\mathcal{G}}-1$ for lattice networks

\mathcal{G}	Exact	Eqn (9)	This work
\mathcal{C}	-0.21875	-0.2181(14)	-0.2187(22)
\mathcal{B}_1	-0.78125	-0.7799(34)	-0.7817(40)
\mathcal{B}_2	-1.34375	-1.3412(54)	-1.3426(82)

TABLE III: Least squares fits of c_n in the square lattice

n_{min}	$n \log (c_n/c_{n-2}) \simeq 2(\gamma-1) + 2n \log \mu_2 + A/n$
10	$0.6870990 + 1.94016321 n - 0.16886256 /n$
20	$0.6870978 + 1.94016321 n - 0.16749947 /n$
30	$0.6870860 + 1.94016321 n - 0.15795150 /n$
40	$0.6870813 + 1.94016321 n - 0.15382565 /n$
50	$0.6870635 + 1.94016322 n - 0.13736803 /n$

the flatPERM algorithm [2, 8, 9, 19] (12 parallel sequences for a total of 2.65×10^9 iterations). In two dimensions $\gamma = 1.34375$ and the $o(1)$ term in equation (3) is believed to be a powerlaw correction of the form $A n^{-1} + B n^{-\Delta}$ (where $\Delta = 3/2$ in two dimensions [3] and is the leading confluent correction exponent).

We use the ratio c_n/c_{n-2} and the model

$$n \log \left(\frac{c_n}{c_{n-2}} \right) \simeq 2(\gamma-1) + 2n \log \mu_2 + A n^{-\Delta_1} \quad (10)$$

to estimate γ . Linear least-squares fits (with $\Delta_1 \in \{0.5, 1.0, 1.5\}$) were done for n greater than or equal to n_{min} where $n_{min} \in \{10, 20, \dots, 100\}$. The results for $\Delta_1 = 1$ and $n_{min} \leq 50$ are shown in table III. For each value of Δ_1 the results were extrapolated against n_{min} using the model $c_0 + c_1/n_{min} + c_2/n_{min}^2$ and comparing the results for the choices of Δ_1 , the estimate

$$\gamma = 1.34359(23) \quad (11)$$

was obtained (the error bar is the largest difference between the average and the estimates). Since $\sigma_1 = (\gamma-1)/2$, this gives

$$\sigma_1 = 0.17188(12), \quad (12)$$

consistent within its error bar with the exact value $\sigma_1 = 0.171875$.

Calculating σ_f for $3 \leq f \leq 6$

An f -star is grown by the GARM algorithm [20] by adding steps to the endpoints of the arms in a cyclic order. The algorithm is an approximate enumeration algorithm, and it estimates numbers $u_n^{(f)}$ of f -stars of length n . To relate $u_n^{(f)}$ to $s_n^{(f)}$ equation (4), first note that the algorithm imposes ordering of the arms: it adds a step to the first arm, then the second arm, and so on. This shows that $u_n^{(f)}$ is the number of f -stars with *labelled*

arms (while $s_n^{(f)}$ is the number of f -stars with unlabelled arms). To determine the symmetry factor relating $s_n^{(f)}$ and $u_n^{(f)}$, note that a monodisperse f -star of length n has k arms of length $\lceil n/f \rceil$ and $f-k$ arms of length $\lfloor n/f \rfloor$. Since the k longest arms can be ordered in $k!$ ways, and the $f-k$ shortest arms in $(f-k)!$ ways, a symmetry factor of $k!(f-k)!$ is introduced. This is particularly true for 3-stars and 4-stars in the cubic lattice, so if $n = mf+k$, then by equation (4) the algorithm estimates the numbers

$$u_n^{(f)} = k!(f-k)! C_k^{(f)} n^{\gamma_f-1} \mu_2^n (1 + o(1)). \quad (13)$$

for $f = 3$ or $f = 4$ in the square lattice. The $o(1)$ correction contains, in addition to analytic and confluent correction terms, parity effects due to the lattice and the number of arms. Our results show that the parity effects decay quickly with increasing n .

Similar arguments for 5- and 6-stars give

$$u_n^{(f)} = V_k^{(f)} s_n^{(f)} \quad (14)$$

where $n = mf+k$ (excluding the extra edge between the two central nodes), and where the symmetry factor is given by

$$V_k^{(f)} = \begin{cases} \lfloor f/2 \rfloor! (3-k)! k!, & \text{if } 0 \leq k < 3; \\ 3! (f-k)! (k-3)!, & \text{if } 3 \leq k \leq f-1. \end{cases} \quad (15)$$

Estimating σ_f numerically for $3 \leq f \leq 6$

Square lattice f -stars for $3 \leq f \leq 6$ were sampled a total of 4×10^9 started flatGARM [20] sequences along 4 parallel threads for lengths up to 1,000 steps per branch (arm). These simulations produced estimates of $u_n^{(f)}$ in equations (13) and (14).

To estimate γ_f-1 from our data, notice that if $x = \gamma_f-1$, then

$$Q_n(x) = \log \left(\frac{u_n^{(f)}}{\mu_d^n n^x} \right) \simeq C_0 + C_1 n^{-1}, \quad (16)$$

where $x = \sigma_f + f\sigma_1$. By using the best estimate of μ_2 in the literature ($\mu_2 = 2.63815853035(2)$ [4]), we determine that value of x so that $Q_n(x)$ approaches a constant as n increases.

In figure 3 $Q_n(x)$ is plotted against $\log_{10} n$ for range of values of x . Note that if $Q_n(x)$ is a constant, then it will present as a horizontal line in this graph, and this will give the optimal value of x . Introduce a minimum cut-off n_{min} on the length of f -stars, and determine the optimal value $\xi_{n_{min}}$ for x as described in the caption of figure 3. This estimate $\xi_{n_{min}}$ is a function of n_{min} . Plotting it gives the graph in figure 4 (where parity effects quickly die down with increasing n). It only remains to

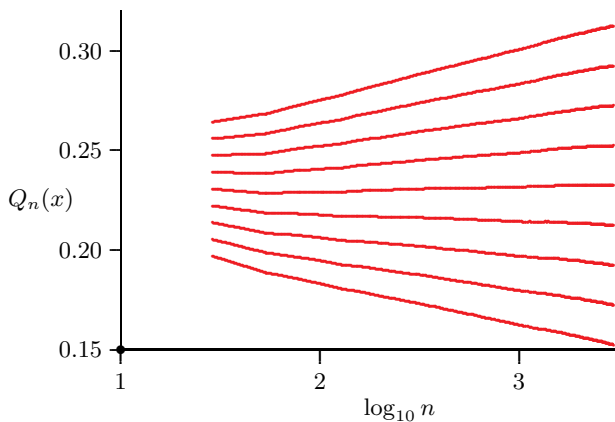


FIG. 3: $Q_n(x)$ for square lattice 3-stars as a function $\log_{10} n$ for $n \geq n_{min}$ and for $x = 0.061565 + 0.0025 m$ where $-4 \leq m \leq 4$. By calculating the average slope or incline of these curves using linear fits, and then interpolating to find that value x which gives a zero average slope or incline, the optimal value of x at this given value of n_{min} (denoted by $\xi_{n_{min}}$) is determined. In this plot, $n_{min} = 30$ and the optimal value of x is $\xi_{30} \approx 0.06249$

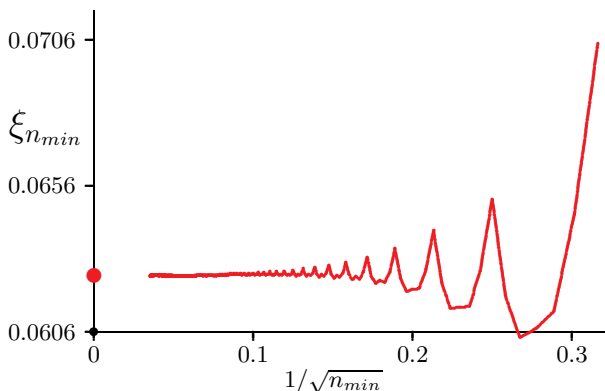


FIG. 4: The estimates of $\xi_{n_{min}}$ for square lattice 3-stars as a function of n_{min} . Notice that parity effects die down quickly. By extrapolating to $n_{min} = \infty$, our best estimate of $\gamma_f - 1$ is obtained (denoted by the bullet on the y -axis).

extrapolate as $n_{min} \rightarrow \infty$. This is done by using the model

$$\xi_{n_{min}} = (\gamma_f - 1) + \frac{A}{\sqrt{n_{min}}} + \frac{B}{n_{min}}. \quad (17)$$

where $250 \leq n_{min} \leq 400$. In the case of 3-stars this gives the estimate $\gamma_3 - 1 \approx 0.06282$.

An error bar is determined by resampling the $\xi_{n_{min}}$. Each point in figure 4 is dropped with probability 0.5 giving a smaller set of estimates. Extrapolating this to determine $\gamma_f - 1$ using the more general model

$$\xi_{n_{min}} = (\gamma_f - 1) + \frac{A}{n_{min}^{1/2}} + \frac{B}{n_{min}^1} + \frac{C}{n_{min}^{3/2}} + \frac{D}{n_{min}^2} \quad (18)$$

gives a degraded estimate of $\gamma_f - 1$ which is dependent on the resampling of the $\xi_{n_{min}}$. Repeating this a large number of times gives a distribution of estimates of $\gamma_f - 1$

which is dependent on noise and systematic errors in our data sets. The variance of this distribution is larger than the (unknown) variance in our best estimate (since each estimate in the distribution is obtained by discarding data). By taking the square root to obtain a standard deviation, and then doubling the standard deviation, an estimated error bar is obtained. The data in figure 4 gives the estimate $\gamma_3 - 1 = 0.06282(33)$. Repeating this analysis for the other f -stars gives the estimated exponents in table IV.

TABLE IV: Estimates of $\gamma_f - 1$ in the square lattice

$\gamma_f - 1$	Exact value	This work
$\gamma_3 - 1$	-0.0625	-0.06282(33)
$\gamma_4 - 1$	-0.5	-0.4989(23)
$\gamma_5 - 1$	-1.34375	-1.3422(13)
$\gamma_6 - 1$	-2.46875	-2.4668(19)

Equations (5) and (12) can now be used to determine the vertex exponents σ_f in table I. We can also improve on these estimates by using the exact value of σ_1 instead of the estimate in equation (12). This gives the estimates in table V.

TABLE V: Vertex exponents in 2 dimensions

f	Exact	[28]	This work
σ_3	-0.453125	-0.45(2)	-0.45281(33)
σ_4	-1.1875	-1.17(4)	-1.1864(23)
σ_5	-2.203125	-2.14(4)	-2.2016(13)
σ_6	-3.5	-3.36(5)	-3.4981(19)

Estimating $\gamma_g - 1$ for uniform trees

In this section the entropic exponents γ_g for uniform lattice trees with connectivities shown in figure 1 are estimated. Self-avoidance in these models induces a repulsive force between nodes of degrees larger or equal to 3 in uniform trees, and this stretches the branches (self-avoiding walks) joining them. This effect may be more difficult to simulate with GARM, and motivated the use of the Wang-Landau algorithm [25] instead. In this study we used a parallel implementation of this algorithm.

We grew branched structures by first growing a central uniform star, and then growing additional branches from the endpoints of the completed arms of the central star. The implementation of the Wang-Landau algorithm grows f -stars by first fixing a central node. The f arms are grown by sampling f edges at the endpoints of the arms and appending them to the star. If it is self avoiding then the state is updated and accepted, and the density is updated. If it is not self avoiding, then the updated state is rejected, the current state is read again, and the density is updated accordingly.

When the star is fully grown a new (secondary) node is chosen uniformly at random from the f endpoints of the lattice star. Once the secondary node is chosen the remaining branches are grown from it analogously to the arms of the star.

Let b denote the number of total branches (including the original star arms), each of length ℓ , of the comb or brush under consideration. The process of first growing a star and then growing the remaining branches is iterated so that each structure of uniform length $n = b\ell$ is independently sampled via the Wang-Landau algorithm for $\ell = 1, \dots, 200$. For each ℓ , on the order of 10^9 configurations were sampled. The implementation was done in parallel by growing uniform trees in separate CPU threads using omp protocols. These threads interacted to control the density update in the Wang-Landau algorithm. As with the parallel implementation of PERM [2], this improved performance of the algorithm.

As in the case of the parallel GARM sampling of stars, a symmetry factor is introduced by the algorithm. If $t_n(\mathcal{G})$ is the number of uniform square lattice combs or brushes of total length n with b arms of length ℓ (so that $n = b\ell$), then the algorithm returned estimates of $v_n(\mathcal{G}) = (b-f)!(f-1)!t_n(\mathcal{G})/(4^{2f-b})$. By equation (7),

$$v_n(\mathcal{G}) = S_{f,b} t_n(\mathcal{G}) = S_{f,b} C_{\mathcal{G}} n^{\gamma_{\mathcal{G}}-1} \mu_2^n (1 + o(1)) \quad (19)$$

where $S_{f,b} = (b-f)!(f-1)!/(4^{2f-b})$. Estimates of $\gamma_{\mathcal{G}}-1$ can be made by analysing these data.

Estimating $\gamma_{\mathcal{G}}-1$ for \mathcal{C}_1 , \mathcal{B}_1 and \mathcal{B}_2

We use a similar approach as for stars (see equation (16)) by determining the value of x so that

$$P_n(x) = \log \left(\frac{v_n(\mathcal{G})}{\mu_2^n n^x} \right) \simeq C_0 + C_1 n^{-1}, \quad (20)$$

where $x = \gamma_{\mathcal{G}}-1$. To account for corrections due to small networks a cutoff ℓ_{min} was introduced and trees with branches of lengths $\ell < \ell_{min}$ were excluded from the analysis. Repeated fits for a range of values of x gave a sequence of estimates which were interpolated to find that optimal value of x where $P_n(x) \simeq \text{constant}$.

TABLE VIII: Estimated lattice star amplitudes in the square lattice

f	$U^{(f)}$	$C_0^{(f)}$	$C_1^{(f)}$	$C_2^{(f)}$	$C_3^{(f)}$	$C_4^{(f)}$	$C_5^{(f)}$
1	1.164(23)						
3	1.2617(52)	0.21028(86)	0.6309(26)	0.6308(26)			
4	1.2256(78)	0.05107(33)	0.2043(13)	0.3064(20)	0.2043(13)		
5	5.252(17)	0.4377(15)	1.3131(43)	0.4377(15)	1.3131(43)	0.8754(29)	
6	25.190(82)	0.6997(23)	2.0992(68)	2.0992(68)	0.6997(23)	2.0992(68)	2.0992(68)

DISCUSSION

Accurate estimates of lattice star vertex exponents σ_f can only be found if the exponent σ_1 (and thus the en-

These fits were repeated for $\ell_{min} \in \{2, \dots, 15\}$ and then similarly extrapolated against $1/\sqrt{\ell_{min}}$ to determine our best estimate of $\gamma_{\mathcal{G}}$.

In order to determine confidence intervals on our estimates, we resampled our data. We selected 90% of the data to estimate the exponent x . This gave several data sets for each value of ℓ_{min} . Each of these data sets were analysed by dropping randomly one half of the ℓ_{min} and then estimating x . Repeating this gave a distribution of estimates. Doubling the standard deviation of this distribution is our confidence interval. In our particular case 90% of the data were selected 10 times and 50% of the ℓ_{min} were randomly discarded 100 times. This gave a distribution of 1,000 estimates of x over which the variance was computed. The results are shown in table VI. The exact values were calculated using the relations in equation (9).

One may instead use the results in the last column of table VI to determine the σ_f exponents using equation (9). This gives the estimates in table VII where we used the exact value of σ_1 .

The results in tables VI and VII shows (numerically) that the vertex exponents σ_f , as related to uniform trees via equation (9), are consistent. In other words, this is strong numerical evidence that the results in equation (8) are correct, at least when applied to monodisperse, acyclic, branched polymers.

TABLE VI: Estimates of $\gamma_{\mathcal{G}}-1$ in the square lattice

$\gamma_{\mathcal{G}}-1$	Exact value	This work
$\gamma_{\mathcal{C}}-1$	-0.21875	-0.2187(22)
$\gamma_{\mathcal{B}_1}-1$	-0.78125	-0.7817(40)
$\gamma_{\mathcal{B}_2}-1$	-1.34375	-1.3426(82)

TABLE VII: Vertex exponents from uniform trees

σ_f	Exact	Table V	from $\gamma_{\mathcal{G}}-1$
σ_3 (via \mathcal{C})	-0.453125	-0.45281(33)	-0.4531(11)
σ_4 (via \mathcal{B}_1)	-1.1875	-1.1864(23)	-1.1880(51)
σ_4 (via \mathcal{B}_2)	-1.1875	-1.1864(23)	-1.1869(41)

tropic exponent γ of self-avoiding walks) is known with sufficient accuracy. We estimated γ in equation (11), and

this compares well with the exact value $43/32 = 1.34375$. This, together with our numerical results for square lattice stars, show compelling evidence that the exact (but not rigorously proven) values of the vertex exponents [5, 15, 16] are correct. In addition, our data on uniform trees show that the relations in equation (9) are satisfied to high accuracy, providing evidence that the scaling relation in equation (8) is correct as well. Overall, our results show that the exact values of the vertex exponents and the conjectured relations for monodispersed acyclic branched networks in equation (9) are consistent.

In addition to estimating the vertex exponents, we also analysed our data to estimate the amplitudes C and C_k^f in equations (3) and (4). The amplitude C in equation (3) is the amplitude of self-avoiding walks. In the case of f -stars, $C_k^{(f)}$ is estimated taking the symmetry factors in equations (13) and (15) into account. Defining $U^{(f)} = k!(f-k)!C_k^{(f)}$ for $3 \leq f \leq 4$, and $U^{(f)} = V_k^{(f)}C_k^{(f)}$ for $5 \leq f \leq 6$, our data show that asymptotically $U^{(f)}$ is independent of the parity class (see, for example, figure 4, where parity effects decreases quickly with increasing n_{min}).

In order to estimate $U^{(f)}$, we used the log-ratio models

$$\log \left(\frac{u_n^{(f)}}{c_n} \right) = \log \left(\frac{U^{(f)}}{C} \right) + B_0 \log n + \frac{C_0}{n}, \quad (21)$$

and

$$\log \left(\frac{u_n^{(f)}}{\sqrt{c_{2n}}} \right) = \log \left(\frac{U^{(f)}}{2\sigma_1 \sqrt{C}} \right) + B_1 \log n + \frac{C_1}{n}. \quad (22)$$

Linear fits were done for $n \geq n_{min}$ where $n_{min} \in \{10, 20, \dots, 200\}$ and the results were extrapolated using

$$\begin{aligned} \log \left(\frac{U^{(f)}}{C} \right) \Big|_{n_{min}} &\approx \beta_0 + \frac{\beta_1}{n_{min}} + \frac{\beta_2}{n_{min}^2}, \\ \log \left(\frac{U^{(f)}}{2\sigma_1 \sqrt{C}} \right) \Big|_{n_{min}} &\approx \delta_0 + \frac{\delta_1}{n_{min}} + \frac{\delta_2}{n_{min}^2}. \end{aligned} \quad (23)$$

Using the estimate of σ_1 in table I, one can solve simultaneously for $\{U^{(f)}, C\}$. The amplitudes $C_k^{(f)}$ are then estimated from the value of $U^{(f)}$. The results are shown in table VIII, where $U^{(1)} \equiv C$ is the self-avoiding walk amplitude. Notice that the estimates for $f = 5$ and $f = 6$ appear to break the trend set by amplitudes for $f \leq 4$. This is due to the different style central nodes in 5-stars and 6-stars, as shown in figure 2.

The amplitudes for the lattice networks were similarly estimated using models like those in equations (21) and (22), and then extrapolated similarly to equation (23). Taking into account the symmetry factors, the results in table IX were obtained.

TABLE IX: Estimates of $C(\mathcal{G})$ and C in the square lattice.

Uniform tree	$C_{\mathcal{G}}$	C
$\mathcal{G} = \mathcal{C}$	0.404(66)	1.186(92)
$\mathcal{G} = \mathcal{B}_1$	0.164(69)	1.187(98)
$\mathcal{G} = \mathcal{B}_2$	0.071(28)	1.191(39)

Acknowledgements

EJJvR acknowledges financial support from NSERC (Canada) in the form of Discovery Grant RGPIN-2019-06303. SC acknowledges the support of NSERC (Canada) in the form of an Alexander Graham Bell Canada Graduate Scholarship (Application No. CGSD3-535625-2019).

-
- [1] J Batoulis and K Kremer. Thermodynamic properties of star polymers: Good solvents. *Macromolecules*, 22:4277–4285, 1989.
 - [2] S Campbell and EJ Janse van Rensburg. Parallel PERM. *J Phys A: Math Theo*, 2020.
 - [3] S Caracciolo, AJ Guttmann, I Jensen, A Pelissetto, AN Rogers, and AD Sokal. Correction-to-scaling exponents for two-dimensional self-avoiding walks. *J Stat Phys*, 120:1037–1100, 2005.
 - [4] N Clisby and I Jensen. A new transfer-matrix algorithm for exact enumerations: self-avoiding polygons on the square lattice. *J Phys A: Math Theo*, 45:115202, 2012.
 - [5] B Duplantier. Polymer network of fixed topology: Renormalization, exact critical exponent γ in two dimensions, and $d = 4 - \epsilon$. *Phys Rev Lett*, 57:941–944, 1986.
 - [6] B Duplantier. Statistical mechanics of polymer networks of any topology. *J Stat Phys*, 54:581–680, 1989.
 - [7] B Duplantier and AJ Guttmann. Statistical mechanics of confined polymer networks. *J Stat Phys*, 180:1061–1094, 2020.
 - [8] P Grassberger. Pruned-enriched Rosenbluth method: Simulations of θ polymers of chain length up to 1,000,000. *Phys Rev E*, 56:3682–3693, 1997.
 - [9] H-P Hsu and P Grassberger. A review of Monte Carlo simulations of polymers with PERM. *J Stat Phys*, 144:597–637, 2011.
 - [10] H-P Hsu, W Nadler, and P Grassberger. Scaling of star polymers with 1-80 arms. *Macromol*, 37:4658–4663, 2004.
 - [11] JC Le Guillou and J Zinn-Justin. Critical exponents for the n -vector model in three dimensions from field theory. *Phys Rev Lett*, 39:95, 1977.
 - [12] JEG Lipson, SG Whittington, MK Wilkinson, JL Martin, and DS Gaunt. A lattice model of uniform star polymers. *J Phys A: Math Gen*, 18:L649–473, 1985.
 - [13] A Miyake and KF Freed. Excluded volume in star polymers: Chain conformations space renormalization group. *Macromolecules*, 16:1228–1241, 1983.
 - [14] A Miyake and KF Freed. Internal chain conformations of star polymers. *Macromolecules*, 17:678–683, 1984.
 - [15] B Nienhuis. Exact critical point and critical exponents of $o(n)$ models in two dimensions. *Phys Rev Lett*, 49:1062–

- 1065, 1982.
- [16] B Nienhuis. Two-dimensional critical phenomena and the Coulomb Gas. In C Domb and JL Lebowitz, editors, *Phase Transitions and Critical Phenomena*, volume 11. Academic Press, London, 1987.
- [17] K Ohno. Scaling theory and computer simulation of star polymers in good solvents. *Cond Mat Phys*, 5:15–36, 2002.
- [18] K Ohno and K Binder. Monte Carlo simulation of many-arm star polymers in two-dimensional good solvents in the bulk and at a surface. *J Stat Phys*, 64:781–806, 1991.
- [19] T Prellberg and J Krawczyk. Flat histogram version of the pruned and enriched Rosenbluth method. *Phys Rev Lett*, 92:120602, 2004.
- [20] A Rechnitzer and EJ Janse van Rensburg. Generalized atmospheric Rosenbluth methods (GARM). *J Phys A: Math Theo*, 41:442002, 2008.
- [21] L Schäfer, C von Ferber, U Lehr, and B Duplantier. Renormalization of polymer networks and stars. *Nucl Phys B*, 374:473–495, 1992.
- [22] CE Soteros. Lattice models of branched polymers with specified topologies. *J Math Chem*, 1:91–102, 1993.
- [23] CE Soteros and SG Whittington. Polygons and stars in a slit geometry. *J Phys A: Math Gen*, 21:L857–L861, 1988.
- [24] CE Soteros and SG Whittington. Lattice models of branched polymers: Effects of geometrical constraints. *J Phys A: Math Gen*, 22:5259–5270, 1989.
- [25] F Wang and DP Landau. Efficient, multiple-range random walk algorithm to calculate the density of states. *Phys. Rev. Lett.*, 86:2050–2053, Mar 2001.
- [26] SG Whittington, JEG Lipson, MK Wilkinson, and DS Gaunt. Lattice models of branched polymers: Dimensions of uniform stars. *Macromol*, 19:1241–1245, 1986.
- [27] SG Whittington and CE Soteros. Uniform branched polymers in confined geometries. *Macromol Rep*, 29(S2):195–199, 1992.
- [28] MK Wilkinson, DS Gaunt, JEG Lipson, and SG Whittington. Lattice models of branched polymers: Statistics of uniform stars. *J Phys A: Math Gen*, 19:789–796, 1986.
- [29] L Zhan. A parallel implementation of the Wang-Landau algorithm. *Comp Phys Commun*, 179(5):339–344, 2008.
- [30] C Zhou and RN Bhatt. Understanding and improving the Wang-Landau algorithm. *Phys Rev E*, 72(2):025701, 2005.
- [31] C Zhou and J Su. Optimal modification factor and convergence of the Wang-Landau algorithm. *Phys Rev E*, 78(4):046705, 2008.